AD-A155 475 ABSORPTION AND SCATTERING PROPERTIES OF AEROSOLS OF AGGREGATED PARTICLES I.. (U) LITTLE (ARTHUR D) INC CAMBRIDGE MA J R ARONSON ET AL. 30 APR 85 1/1

UNCLASSIFIED ARO-17753.2-GS DAAG29-82-C-0006 F/G 20/6 NL

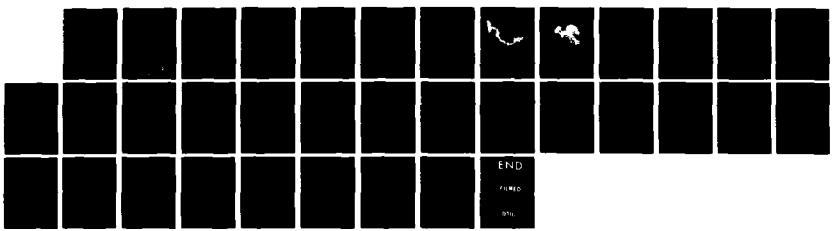

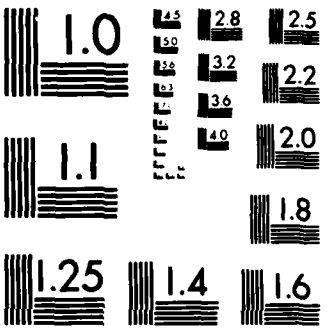

MICROCOPY RESOLUTION TEST CHART
NATIONAL BUREAU OF STANDARDS-1963-A

ABSORPTION AND SCATTERING PROPERTIES OF AEROSOLS OF AGGREGATED PARTICLES IN THE INFRARED SPECTRAL REGION

BY

JAMES R. ARONSON, IVAN SIMON AND EMMETT M. SMITH

APRIL 30, 1985

U.S. ARMY RESEARCH OFFICE

CONTRACT DAAG29-82-C-0006

ARTHUR D. LITTLE, INC.

APPROVED FOR PUBLIC RELEASE;
DISTRIBUTION UNLIMITED

UNCLASSIFIED

SECURITY CLASSIFICATION OF THIS PAGE (When Data Entered)

REPORT DOCUMENTATION PAGE		READ INSTRUCTIONS BEFORE COMPLETING FORM
1. REPORT NUMBER ARO 17753.2-GS	2. GOVT ACCESSION NO.	3. RECIPIENT'S CATALOG NUMBER
4. TITLE (and Subtitle) ABSORPTION AND SCATTERING PROPERTIES OF AEROSOLS OF AGGREGATED PARTICLES IN THE INFRARED SPECTRAL REGION		5. TYPE OF REPORT & PERIOD COVERED FINAL 4/82 - 4/85 6. PERFORMING ORG. REPORT NUMBER
7. AUTHOR(s) James R. Aronson, Ivan Simon and Emmett M. Smith		8. CONTRACT OR GRANT NUMBER(s) DAAG29-82-C-0006
9. PERFORMING ORGANIZATION NAME AND ADDRESS Arthur D. Little, Inc. Acorn Park Cambridge, Mass. 02140		10. PROGRAM ELEMENT, PROJECT, TASK AREA & WORK UNIT NUMBERS
11. CONTROLLING OFFICE NAME AND ADDRESS U. S. Army Research Office Post Office Box 12211 Research Triangle Park, NC 27709		12. REPORT DATE 4/30/85 13. NUMBER OF PAGES 30
14. MONITORING AGENCY NAME & ADDRESS(if different from Controlling Office)		15. SECURITY CLASS. (of this report) Unclassified 15a. DECLASSIFICATION/DOWNGRADING SCHEDULE

16. DISTRIBUTION STATEMENT (of this Report)

Approved for public release; distribution unlimited.

17. DISTRIBUTION STATEMENT (of the abstract entered in Block 20, if different from Report)

NA

18. SUPPLEMENTARY NOTES

The view, opinions, and/or findings contained in this report are those of the author(s) and should not be construed as an official Department of the Army position, policy, or decision, unless so designated by other documentation.

19. KEY WORDS (Continue on reverse side if necessary and identify by block number)

Aerosols, Aggregates, Soot, Photoacoustic measurements, Theory of Absorption and Scattering

20. ABSTRACT (Continue on reverse side if necessary and identify by block number)

This report concerns the extension of a theory of particulate scattering to the difficult case of aggregated aerosols. Photoacoustic measurements of absorption and scattering in the infrared and visible spectral regions have been made for SiO_2 and C smokes to test the validity of the theory.

DD FORM 1 JAN 73 1473 EDITION OF 1 NOV 65 IS OBSOLETE

UNCLASSIFIED

SECURITY CLASSIFICATION OF THIS PAGE (When Data Entered)

TABLE OF CONTENTS

LIST OF ILLUSTRATIONS AND TABLES

I. Introduction

The development of suitable screening materials for infrared radiation, particularly in the 3-5 μm and 8-13 μm regions is required by developments of modern infrared detection technology. Such smokescreen materials derive their value from either absorption or scattering phenomena or some combination of the two. Because scattering phenomena may be optimized with regard to wavelength of effective operation by suitable choice of particle size and refractive index, the corrollary is also true: viz. no one scattering material is likely to be equally valuable over all wavelengths. Thus, if it is desired to develop scattering aerosols for smokescreens that will be effective in the thermal infrared region, it is also likely that they will not work very efficiently in the visible region. It is obvious that to produce an infrared smokescreen which does not at the same time provide conventional protection in the visible region is an unsatisfactory development. It is of course true that separate smokescreen materials could be used for each of the relevant electromagnetic wavelengths, but it would be much better to be able to provide a single smokescreen for use over a broad spectral range.

Absorption phenomena, on the other hand, have the possibility of being applicable over a wide range of wavelengths providing suitable materials are chosen. However, the list of materials exhibiting such a

wide range absorption is limited to those containing free electrons, as bound electrons have different resonant frequencies and are therefore best suited to screening in particular wavelength regions. Most free electron compounds (e.g. many metals) tend to be pyrophoric when produced in small particle size and therefore are not suitable. However, one well-known stable class of materials has both free electron based absorption, effective over a wide spectral range, and is easily produced. We refer to carbon based materials such as soots.

Unfortunately, the extinction properties of carbon based materials are poorly understood for several reasons. Different soot materials, being somewhat variable chemically, have differing optical constants. Furthermore, their structures tend to be quite complicated as can be seen in Figures I-1 and I-2.

These substances are examples of a class of materials for which the optical properties are insufficiently understood. They are inhomogeneous on a microscopic scale and yet relatively homogeneous at the scale imposed by the radiation wavelengths in which we are interested. As such they are candidates for optical modeling using Effective Medium type theories.

As can be inferred from the electron photomicrographs the detailed geometry of such aggregates is quite difficult to model. Nonetheless in view of the inapplicability of standard Mie theory type treatments, we chose to conduct an investigation of the applicability to aggregate

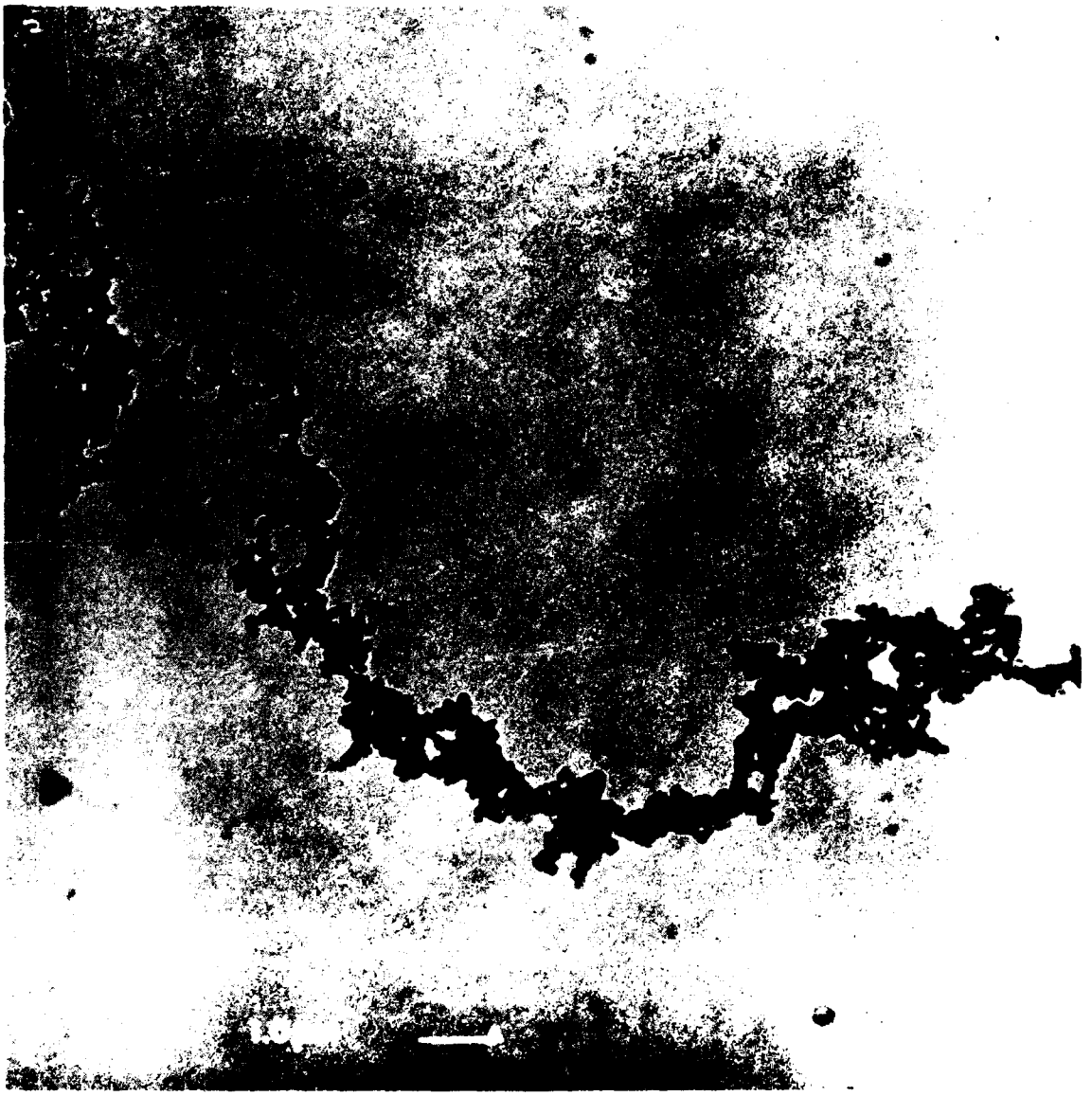

FIGURE I-1

Chain-like Soot Electron Photomicrograph

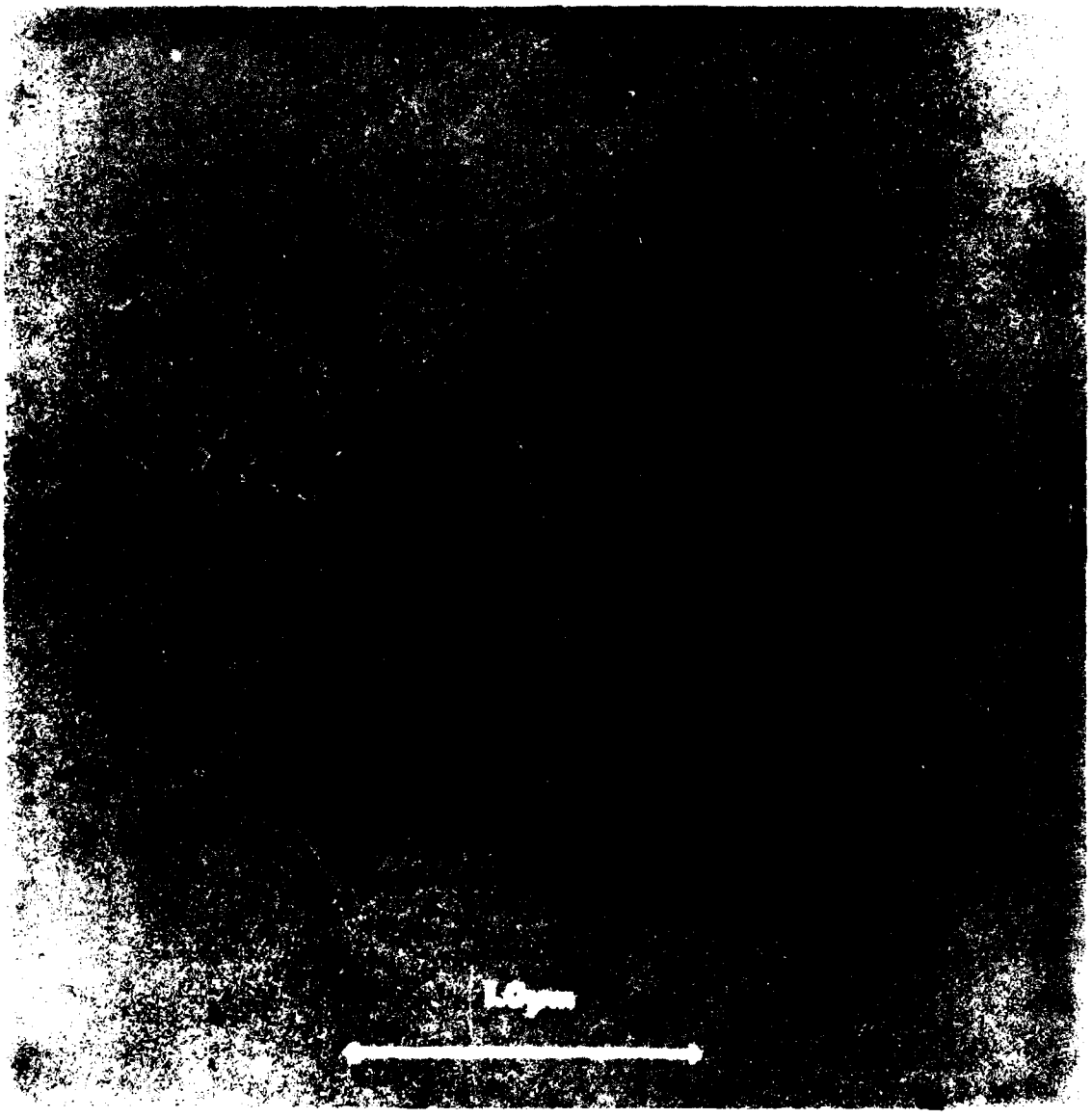

FIGURE I-2

Cluster Soot Electron Photomicrograph

aerosols of a more statistical theory of absorption and scattering by irregularly shaped particles.

To ascertain the validity of our treatment we made photoacoustic measurements on such aerosols in the infrared and visible spectral regions. As will be described below the measurements were made using a line-by-line tuneable CO_2 laser operating in the 9-11 μm region and a three wavelength (0.633, 1.15, 3.39 μm) He Ne laser. These lasers were chosen so as to provide measurements in the principal infrared regions of atmospheric transparency, 3-5μm and 8-13μm. In addition, a measurement in the visible region was desired to be able to compare our work with that reported previously by other scientists. A near infrared measurement in the region of the militarily important YAG lasers was also considered useful.

Much of the effort on this project involved setting up the experimental systems, making various calibrations, choosing the appropriate smoke generator parameters, exploring various options for data reduction and particle characterization and making sufficient experimental runs to eliminate spurious effects. The results of our work were presented at the 1984 CRDC Scientific Conference on Obscuration and Aerosol Research in June 1984 at the Edgewood Area, Aberdeen Proving Ground, Maryland. The paper from the proceedings of that conference describes the body of our work. It is included in this report in the following section.

Absorption and Scattering by Aggregated Aerosol Particles

by

J. R. Aronson, A. G. Emslie, I. Simon and E. M. Smith
Arthur D. Little, Inc.
Cambridge, Massachusetts 02140

ABSTRACT

This paper concerns the extension of a theory of particulate scattering to the difficult case of aggregated aerosols. Photoacoustic measurements of absorption and scattering in the infrared and visible spectral regions have been made for SiO_2 and C smokes to test the validity of the theory. This work was presented as:

J. R. Aronson, A. G. Emslie, I. Simon and E. M. Smith,
"Scattering and Absorption by Aggregated Aerosol Particles,"
1984 CRDC Conference on Obscuration and Aerosol Research, June 1984.

This is a progress report. Further measurements and refinements are continuing.

I. INTRODUCTION

The problem of scattering and absorption by particles is presently well understood in terms of Mie theory for spheres and similarly for cylinders[1] and spheroids[2]. There is presently considerable work going on utilizing more approximate methods for irregularly shaped particles[3]. Roessler and Faxvog have investigated the absorption and scattering of carbon smokes[4,5] and found that the Mie theory could adequately explain scattering and absorption by smoke particles (which are believed to be largely chained aggregates) by treating them as spheres if one worked only at visible wavelengths. However, attempts at treating infrared measurements by the same method failed.

We concluded that a viable approach to the problem of scattering by aggregated aerosols might be made by treating the aggregate as an individual particle having effective-medium optical constants[6] established by the optical constants of the material and its volume fraction within the aggregate. A similar approach had been previously used by us for fine particle soils with some success[7]. We then proposed that the gross characteristics of the aggregate could be handled by our previously developed theory[8,9] in much the same way as we had handled irregularly shaped particles in the past. In order to guide and validate the theoretical treatment we proposed to use photoacoustic spectroscopy with

He-Ne and CO_2 laser sources operating in the visible, near-infrared and mid-infrared spectral regions. The reason for the choice of the photoacoustic method was principally that it permits one to obtain a scattering coefficient without the use of an integrating sphere, as would be necessary with standard infrared methods.

II. THEORETICAL APPROACH

Our previous theoretical treatment has been described in the literature quite fully[8,9]. We needed to modify our theory in several minor ways, however. As most of the particles are small compared to the wavelengths in question (infrared) we only modified our fine particle theory, which for globular aggregates consists of a Raleigh scattering calculation using the effective optical constants of the medium. For fibers we used our treatment described previously[10] if the length of the fiber was not small compared to the wavelength and our usual treatment[8,9] if all dimensions of the fiber were small. As we rarely have fibers larger than the wavelength we only needed to implement this portion of the computer program for those fibers which fell within the region to be bridged by the two theories. As shown in our previous work, bridging is useful in the intermediate region; therefore, a bridging formula such as the one previously used[11] was also implemented.

III. GENERATION OF AEROSOLS AND ESTIMATION OF THEIR PARAMETERS

The two types of aerosols we studied in this work were acetylene-flame smoke and pyrolytic-silica smoke. Both consist of small primary, nearly spherical particles of the pure substance (carbon, silicon dioxide) coagulated into larger aggregates of various configurations.

A. Acetylene Smoke Generator

The apparatus used to generate the carbon aerosol is similar to that described by Roessler[5]. Acetylene is mixed with air in a closely controlled proportion in a burner with a 1.0 mm dia. orifice mounted in a vertical chamber of ∿15 cm diameter and ∿ 90 cm height. The laminar flame is approximately 15 to 20 cm high and under proper conditions (around ∿ 0.5 air-to-gas ratio by volume) produces dense carbon aerosol throughout the chamber. Some of it is lead from the chamber into the photoacoustic cell and to the sampling filter (Nucleopore, 0.1 μm pore size) for subsequent electron microscope examination. The aerosol could be diluted, if necessary, by air added to the stream.

B. Silica Smoke Generator

The apparatus used to generate silica aerosol is similar to that described by Kanapilly[12]. Tetraethoxysilane is carried by nitrogen gas from a glass bubbler, mixed with humidified air, and reacted in a quartz tube at 670°C. A dry-ice trap removes condensable reaction products. The aerosol could be diluted with air and a downstream pump causes the aerosol to flow to the photoacoustical cell at a constant rate of about 1 ℓ/min.

C. Smoke Parameter Estimation

In order to carry out our theoretical simulations it is necessary to obtain estimates of the aggregate dimensions and porosity, and number of aggregates per unit volume in the sample space. The former are accomplished by electron microscopy and the latter by weighing collected samples on Nucleopore filters. The latter required about 15 to 20 minutes at a flow rate of 1 ℓ/min. An opacity monitor measuring the optical density of the smoke (in visible light) was used to monitor the rate of carbon aerosol generation. Having calibrated the opacity vs. the gravimetric mass concentration, we were able to use the former in the later runs for estimating the mass concentration without having to collect samples for long time intervals.

We categorize the particles as spheres, ellipsoids and cylinders and measure appropriate dimensions for each. In order to estimate the porosity of the soot particles, we examine the TEM grids from the filter at magnifications of 40 to 120,000. Areas of photographs of these are then selected where we can estimate a volume, count the number of subparticles in it, and thence calculate the porosity. For silica smokes we used the SEM photographs at 5000 magnification both to determine the dimensions of the particles and the dimensions of individual spheres that make up the filamentary particles. We determined that for this we needed to make the measurements using stereo pairs of photographs since the filaments tend to project at various angles from the filter surface.

As a consequence of the well known uncertainty of optical constants for soot[13] we chose to make our experiments with an acetylene-based smoke known to be principally pure carbon, and to use the dispersion theory formulation of Lee and Tien[14] as the best values we could obtain. Clearly, any errors which result from having inappropriate optical constants will be difficult to track down. For silica smokes the problem is less severe, but it does occur, and we chose to try values obtained by Zolotarev[15] and those obtained by Huffman[16]. Somewhat better simulations were obtained using the latter, principally at 10.6 μm.

IV. PHOTOACOUSTIC MEASUREMENTS

The photoacoustic method is particularly suited for the determination of absorption and scattering because the photoacoustic effect arises only from the radiation absorbed by the aerosol particles and converted to heat; the radiation scattered by the particle does not contribute to the acoustic signal. This circumstance makes it possible to separate the two components making up the extinction of the radiation propagating through the aerosol.

The photoacoustic effect[17] is a thermal phenomenon in which periodic heating of a gas manifests itself by corresponding periodic pressure variations detectable by a microphone coupled to the absorption cell. In an aerosol we assume that the heat is generated by absorption of the radiation in the particles only, but is transferred rapidly to the gas, which in itself is perfectly transparent. The condition for rapid heat transfer between the particles and the gas is that the time constant τ for the heat transfer be shorter than the period τ_a of the acoustic frequency used in the experiment. For spherical particles the heat-transfer time constant was obtained by Chan[18] as

$$\tau = a^2 C_p \rho_p / 3 K_a, \tag{1}$$

where a is the radius of the particle, C_p is its specific heat, ρ_p its density and K_a is the thermal conductivity of the air. For carbon particles of radius 1 μm in air we find $\tau \simeq 2 \times 10^{-5}$ sec while the acoustic period at our operating frequency (150 Hz) is $\tau_a \simeq 6.7\ 10^{-3}$ sec. Thus the condition for rapid heat transfer is satisfied and the determination of the absorption from the corresponding photoacoustic signal is undoubtedly valid.

The determination of scattering is somewhat less certain, depending on the assumptions made about the scattering parameters of the particles constituting the aerosol. Basically, it is necessary to determine the total extinction ε and then obtain the scattering by subtracting the absorption from it

$$S = \varepsilon - \alpha. \tag{2}$$

If we assume isotropic scattering we may determine ε either by measuring the optical extinction of a collimated beam of radiation passing through the photoacoustic cell of length L (single path method)

$$\varepsilon_1 = \frac{1}{L} \ln (I_o/I), \tag{3}$$

or by passing the beam through the cell twice (forward and back again) and measuring the two acoustic signals S_1 and S_2

$$\epsilon_2 = \frac{1}{L} \ln [t^2 r S_1/(S_2-S_1)] \quad (4)$$

where t is the transmittance of the cell windows and r is the reflectance of the retroreflecting mirror (double pass method).

The experimental apparatus used in our measurements can be described following the diagram in Figure 1. The photoacoustic cell is a copper tube 1.10 cm I.D., 51.7 cm long, provided with barium fluoride windows (W) inclined at the Brewster angle. The tube is blackened inside to minimize the reflection of scattered radiation. The valves on the cell provide for filling it with the aerosol and for subsequent flushing with dry nitrogen. They are closed during the measurement in order to minimize the acoustic noise. The microphone M picks up the acoustic pressure variations and delivers the signal, via preamplifier PA to the lock-in amplifier LA where it is filtered and synchronously demodulated. The phase reference is derived from the optical chopper which modulates the laser beam at 150 Hz. The photoacoustic cell is operated well below its fundamental resonance frequency ($\sim$320 Hz).

Two lasers can be used alternatively; a Jodon He-Ne laser for operation at three wavelengths: 0.633, 1.15 and 3.39 μm, and a Laakman CO_2 laser, at about 28 wavelengths between 9.27 and 10.63 μm. The waveguide type, rf-excited CO_2 laser is grating tunable and has a beam power output up to $\sim$2 watt (cw). It is stabilized by a cavity servo control system which makes it possible to lock in on any selected line in the 9 to 11 μm vibrational-rotational bands of the CO_2 molecular spectrum. The He-Ne laser is of the dc-plasma discharge type and produces the visible red radiation at 0.633 μm with a $\sim$20 mW (cw) power output. With other sets of cavity mirrors optimized for the infrared emissions it delivers $\sim$6 mW at 1.15 μm and $\sim$8 mW at 3.39 μm.

The CO_2 laser beam has an angular divergence of 3 to 5 millirad (the He-Ne is much less) and is sufficiently narrow to pass through the cell without grazing the walls. However, for the double-pass operation, it is necessary to narrow down the beam which is accomplished by use of a long focal length concave mirror M2. A spurious acoustic signal generated by the laser beam passing through the cell windows was occasionally troublesome, in particular, when the signal from the aerosol was very weak. Therefore, we subtracted the "empty cell" signal from that received from the aerosol.

The laser beam power is measured by a theromopile power meter P, normally placed behind the cell, as shown in Figure 1. For the double-pass measurement the power meter is removed from the beam path. The photoacoustic responsivity of the cell is determined by filling it with an IR absorbing gas

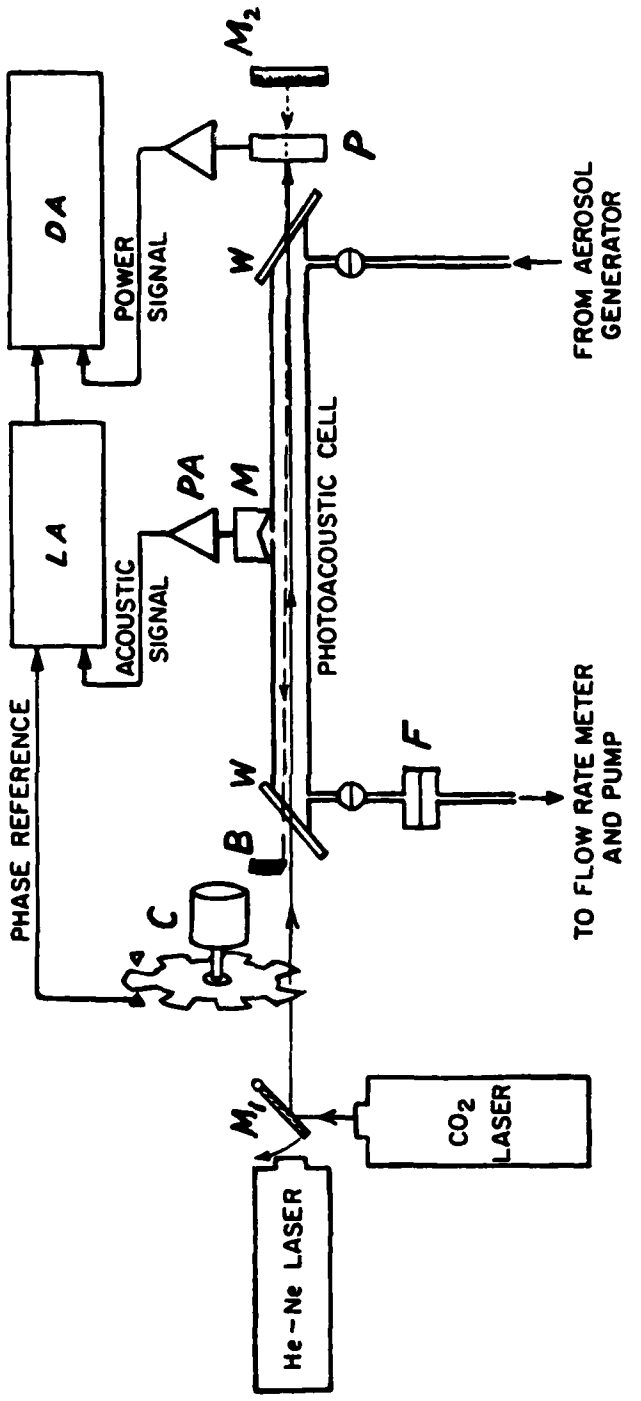

FIGURE 1. SCHEMATIC DIAGRAM OF THE PHOTOACOUSTIC APPARATUS

(ethylene-nitrogen mixture) and measuring the acoustic signal corresponding to a given beam power. The responsivity was, typically ~100 mV/W.

In the course of this work we routinely used both the single and double pass methods for the determination of absorption and scattering coefficients. However, the data presented here were obtained by the conventional single pass method since we found the double pass method to be more susceptible to experimental errors associated with the reverse beam operation.

V. RESULTS

Tables 1 and 2 give a summary of our experimental results together with the measured parameters and theoretical simulations. Simulations have been made for those cases (infrared) in which the theory is believed to be applicable. We did not attempt to model ellipsoids large compared to the wavelength as our objective was to deal with infrared measurements of aerosols, and such large particles are unlikely to remain airborne. The mixtures of shapes that were found in our experiments were modeled by calculating individual absorption coefficients and scattering coefficients (K's and S's) and adding them to get the K's and S's for the mixture. The ratios (K/S) are useful in that errors in estimation of the number of particles cancel out.

The results obtained with carbon aerosols (acetylene smoke) are presented in Table 1. At the 10.5 μm wavelength the theoretical values of the absorption coefficient K are reasonably close to the measured values and their mean value is also close to that obtained from the data of Roessler and Faxvog[4] at 10.6 μm. The calculated values of the scattering coefficients appear to be systematically smaller than the experimental values, but the latter seem to be very close to those obtained from Ref. 4. The experimental K/S ratios are seen to be always smaller (~2 to 3 times) than the theoretical ones. At the 3.39 μm wavelength the only case theoretically modeled is in good agreement with the experiment. The results of measurements in the visible at (0.633 μm) are shown only for general interest and for comparison with literature values. No comparison was made with the theory as that was deemed unwarranted. ($\lambda < D$).

We are uncertain as to the principal causes of the disagreement between the theory and the experiment, but we note that the poorest known parameter is the porosity of the aggregate as this is very difficult to estimate from the TEM and SEM photographs. Figure 2 shows that this parameter can have a very significant effect. For the given specific case K/S can be either greater or less than unity

TABLE 1

CARBON AEROSOL

	AEROSOL PARAMETERS							THEORY			EXPERIMENT		
λ	M	Shape	% Vol.	N	D	ℓ	ρ	K	S	K/S	K	S	K/S
μm	$gcm^{-3} \times 10^{-7}$			$cm^{-3} \times 10^{5}$	μm	μm	=1-fv	$cm^{-1} \times 10^{-4}$			cm^{-1}	$\times 10^{-4}$	
0.63	0.3										27.0	13.3	2.03
0.63	1.46										79.2	32.1	2.47
0.63	1.39										37.7	31.2	1.21
								mean value					1.9
								Roessler & Faxvog, mean(at λ = 0.514)					5.5
1.15	1.6										35.8	18.8	1.90
1.15	2.9										88.1	47.1	1.87
3.39	2.9	ellip.	14	0.37	1.3			5.93	11.5	0.52			
		sph.	9	1.9	0.64			3.63	0.84	4.31			
		cyl.	77	2.7	0.71	2.1	0.50	10.0	4.16	2.40			
								19.6	16.5	1.19	26.7	24.8	1.08
3.39	1.3										10.1	14.8	0.68
3.39	2.0										16.1	16.6	0.97
3.39	3.0										36.9	26.1	1.41

TABLE 1 (Continued)

CARBON AEROSOL

	AEROSOL PARAMETERS							THEORY			EXPERIMENT		
λ	M	Shape	% Vol.	N	D	ℓ	ρ	K	S	K/S	K	S	K/S
μm	$gcm^{-3} \times 10^{-7}$			$cm^{-3} \times 10^{5}$	μm	μm	=1-fv	cm^{-1} x 10^{-4}			cm^{-1}	x 10^{-4}	
10.5	3.3	ellip.	74	4.2	1.5		0.17	4.79	0.394	12.2			
		sph.	17	2.7	1.1			1.21	0.039	30.7			
		cyl.	9	3.6	0.36	2.4		0.16	0.0015	112.4			
								6.16	0.435	14.2	13.0	2.66	4.9
10.5	2.6	ellip.	50	0.93	1.3		0.59	3.86	0.728	5.3			
		sph.	42	1.2	1.1			3.01	0.345	8.7			
		cyl.	8	0.64	0.37	2.4		0.23	0.008	28.7			
								7.10	1.081	6.6	8.07	2.53	3.2
10.5	1.4	ellip.	66	1.4	1.45		0.32	2.68	0.338	7.9			
		sph.	26	3.5	1.06			3.26	0.199	16.4			
		cyl.	8	8.1	0.38	2.4		0.88	0.017	52.6			
								6.82	0.554	12.3	6.08	1.29	4.7

mean value 4.27

Roessler & Faxvog, mean 4.22

Optical Constants: n = 2.64, k = 1.68 at λ = 3.39 μm (Lee & Tien, 1981)
n = 3.78, k = 3.15 at λ =10.5 μm (Lee & Tien, 1981)

TABLE 2

SILICA AEROSOL

	AEROSOL PARAMETERS							THEORY			EXPERIMENT		
λ	M	Shape	% Vol.	N	D	ℓ	ρ	K	S	K/S	K	S	K/S
μm	$gcm^{-3} \times 10^{-7}$			$cm^{-3} \times 10^{5}$	μm	μm	=1-fv	$cm^{-1} \times 10^{-4}$			$cm^{-1} \times 10^{-4}$		
0.633	4.2*	cyl.	100*	11.4*	0.35*	3.1*	0.56*	0.017	20	8.4×10^{-4}	0.28	49.7	56×10^{-4}
9.3	4.8	cyl.	92	13.4	0.34	2.5	0.65	10.2	0.185	55	37	2.3	16.1
10.5	4.2*	cyl.	100	11.4	0.35	3.1	0.56	0.33	0.014	24	11.9	1.2	9.9
10.5	5.4	cyl.	98	19.0	0.36	2.0	0.63	0.45	0.022	20	14.4	2.3	6.3

*) assumed the same as in run indicated below

Optical Constants

$n = 1.46$, $k = 1.16 \times 10^{-4}$ at $\lambda = 0.633$ μm (Dupont Pifax S-220)

$n = 1.9$, $k = 0.05$ at $\lambda = 10.6$ μm)
$n = 2.59$ $k = 2.06$ at $\lambda = 9.3$ μm) Steger, et al. 1974

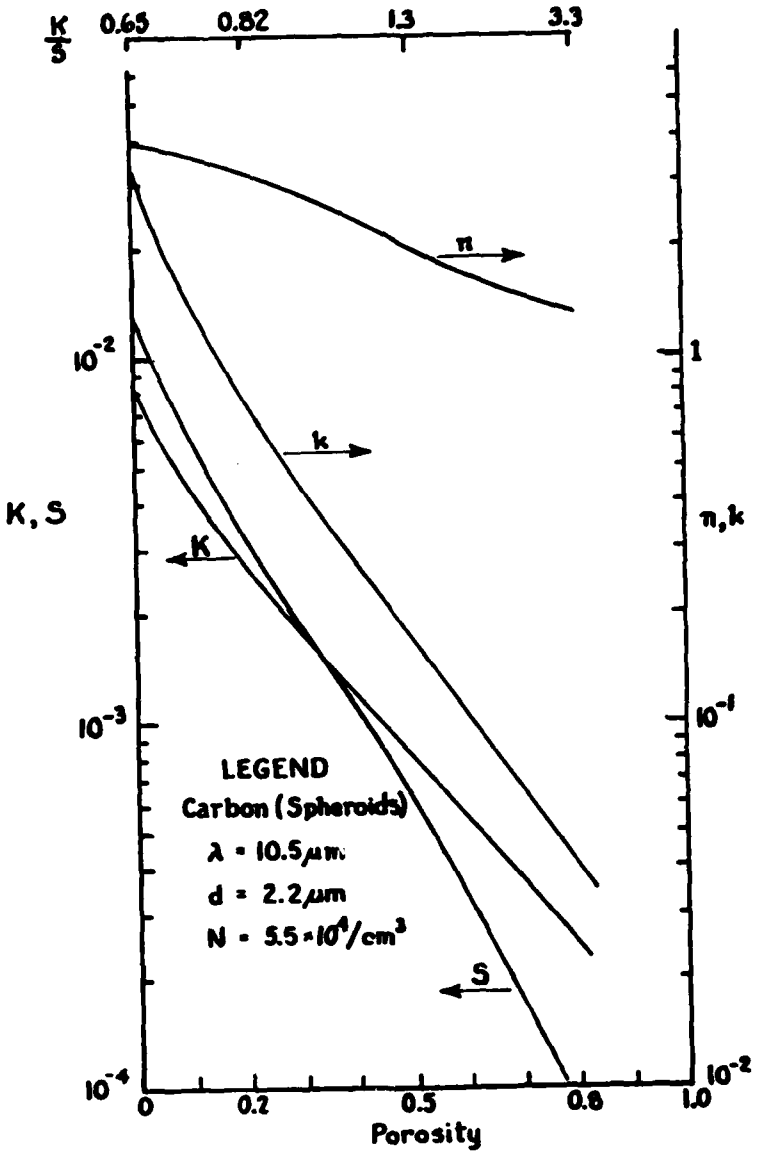

FIGURE 2. EFFECTS OF AGGREGATE POROSITY

depending on whether the porosity of the aggregate is estimated to be greater or less than ~0.3. While our work and most of the literature shows $K > S$ it should be noted that Dugin, et al[19] found the reverse for carbon smoke.

Table 2 summarizes the results obtained with the silica aerosols. The measurements in the infrared were made at 9.3 and 10.5 μm and in both instances the agreement with the theory is reasonably close only for the K/S ratio. The absolute values of K and S seem to be greatly underestimated by the calculation as compared with the experiment (possibly with the exception of the case at $\lambda = 9.3$ μm). In the visible ($\lambda = 0.633$ μm) the theoretical values of both K and K/S are smaller than the experimental ones, contrary to all other cases. It is to be noted that in this case we find $(K/S) << 1$ both by the theory and the experiment in agreement with expectation.

ACKNOWLEDGEMENT

We thank Clark Grain and Fred Johnston for producing the SiO_2 aerosol, Ray Cornish for electron microscopy and Madeline Goode for typing the manuscript. This work was supported by the U.S. Army Research Office.

VI. REFERENCES

1. K. N. Liou, Appl. Opt. 11, 667 (1972).
2. S. Asano and G. Yamamoto, Appl. Opt. 14, 29 (1975)
3. "Light Scattering by Irregularly Shaped Particles," ed by D. W. Schuerman, Plenum Publishing Corp., 1980.
4. D. M. Roessler and F. R. Faxvog, J. Opt. Soc. Am. 69, 1699 (1979).
5. D. M. Roessler and F. R. Faxvog, J. Opt. Soc Am. 70, 230 (1980).
6. C. G. Granqvist and O. Hunderi, Phys. Rev. B 18, 2897 (1978).
7. J. R. Aronson, A. G. Emslie and H. G. McLinden, Science 152, 345 (1966).
8. A. G. Emslie and J. R. Aronson, Appl. Opt. 12, 2563 (1973).
9. J. R. Aronson and A. G. Emslie in "Infrared and Raman Spectroscopy of Lunar and Terrestrial Minerals," Ed. by C. Karr, Jr., Academic Press (1975).
10. J. R. Aronson, A. G. Emslie, F. E. Ruccia, C. R. Smallman, E. M. Smith, and P. F. Strong, Appl. Opt. 18, 2622 (1979).
11. J. R. Aronson and A. G. Emslie, J. Geophys. Res. 80, 4925 (1975).
12. G. M. Kanapilly, K. W. Tu, T. B. Larsen, G. R. Fogel and R. J. Luna, J. Colloid and Interface Sci. 65, 533 (1978).
13. J. T. Twitty and J. A. Weinman, J. Appl. Meteor. 10, 725 (1971).
14. S. C. Lee and C. L. Tien, 18th Symp. on Combustion, The Combustion Institute, 1150-1166 (1981).
15. V. M. Zolotarev, Opt. and Spectrosc. 29, 34 (1970).
16. T. R. Steger, K. L. Day and D. R. Huffman, Appl. Opt. 13, 1586 (1974).
17. "Optoacoustic Spectroscopy and Detection," Ed. by Y. M. Pao, Academic Press (1977).
18. C. H. Chan, App. Phys. Letters 26, 628,(1975).
19. V. P. Dugin, Yu. G. Toporkov and N. V. Zadovina, Izvestiya, Atm. and Oceanic Phys. 17, 728 (1981).

III. Smoke Generators

The two kinds of smokes studied during this project were produced in generators that will be described here in more detail than in the CRDC paper.

A. Acetylene Smoke Generator

The apparatus used to generate the carbon aerosol is shown schematically in Figure III-1. Acetylene is mixed with air at a closely controlled proportion in a burner with a 1.0mm dia. orifice mounted in a vertical chamber of 15 cm diameter and 90 cm height. The laminar flame is approximately 15 to 20 cm high and under proper conditions (around 0.5 air-to-gas ratio by volume) produces dense carbon aerosol throughout the chamber. Some of it is withdrawn through the sampling tube from the chamber into the system.

The flow of the aerosol in the entire system is affected by a suction air pump and controlled by a throttling valve, as shown in the figure. Typically, we used a rate of flow of 1.0 ℓ/min, measured by a rotameter and manually controlled to remain constant during the sampling period. The density of the aerosol is varied by controlling the flow rates of gas and air into the burner and adjusted to a desired level as indicated by an opacity monitor. For very low concentrations, diluent

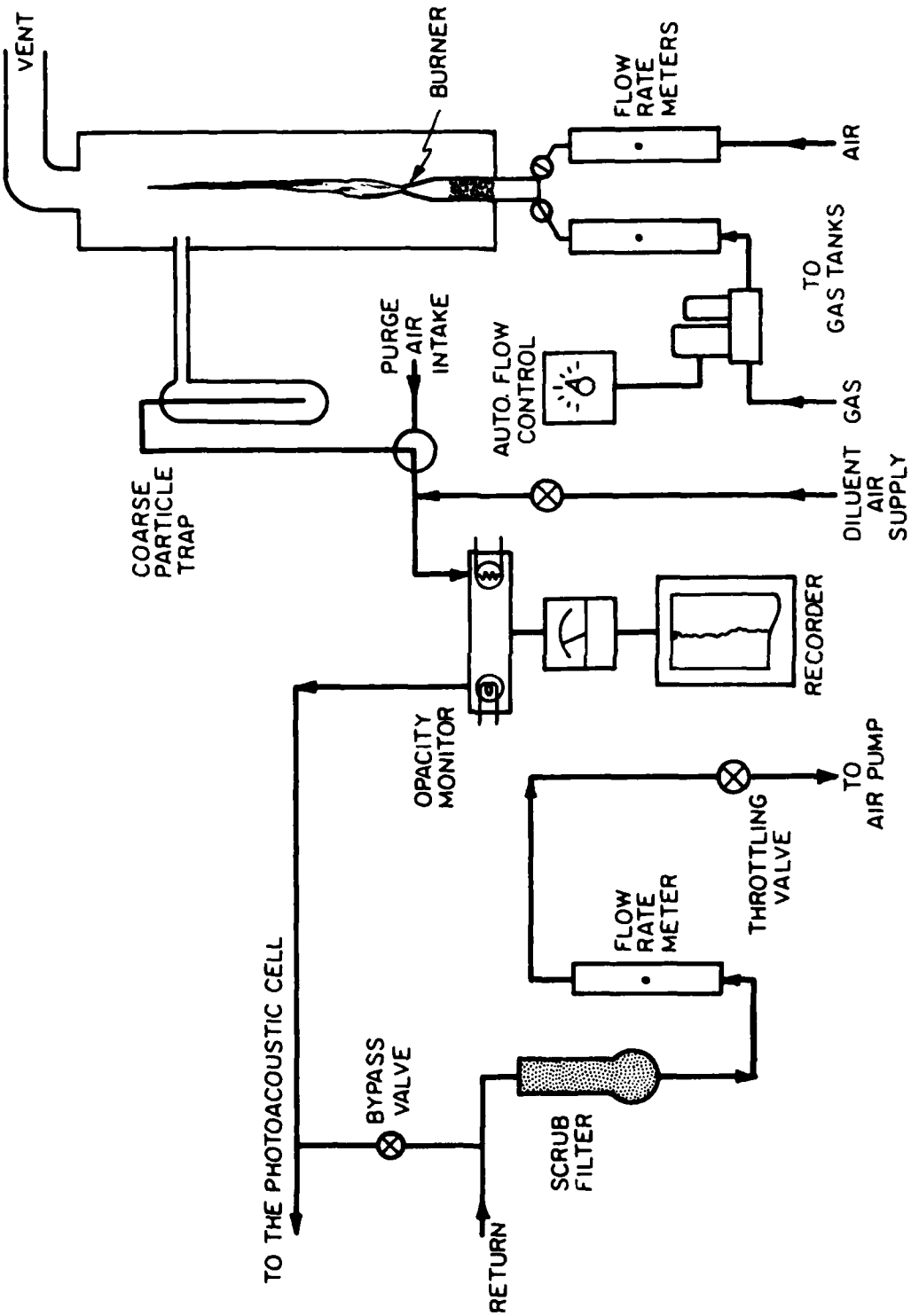

FIGURE III-1 ACETYLENE SMOKE GENERATOR

air is bled into the stream by a needle valve.

The opacity monitor consists of a 15 cm long tube containing a small light bulb at one end and a photoresistive detector at the other, with suitable electronics to produce a voltage approximately proportional to the optical opacity which, in turn, was found by calibration, to be proportional to the mass concentration of carbon in the smoke. We found it necessary to record the opacity during the time of sampling for weight determination on the Nuclepore filter (F in Figure 1 of the preprint) so that appropriate correction could be made for any possible long or short term deviations from the preset level.

The bypass valve shown in Figure III-1 is used during the time the flame is being adjusted to produce aerosol of the desired concentration. By bypassing the flow before the photoacoustic cell we could avoid excessive deposits of carbon in the cell and on its windows. We did provide purging ports at the cell windows but we preferred not to use them for two reasons: first, purging air would tend to dilute the aerosol in the cell by an uncertain amount; second, we found it necessary to make photoacoustic measurements with all flow through the cell shut off in order to minimize the acoustic noise. We cleaned the cell windows before every run and tested their transmittance before and after the run.

We found that, with the exception of very high concentrations of the aerosol (greater than $\sim 5 \times 10^{-7}$ gm cm^{-3}), the deposition of carbon on the windows during the brief time ($\sim$1 min.) of filling the cell was negligible. At any rate, the actually measured value of the transmittance of the cell windows was included in the evaluation of the photoacoustic signals (Eq. 4) and a correction for a background signal caused by the deposit on the windows was made.

Once the cell was filled and closed the aerosol settled under gravity and the photoacoustic signal was seen to diminish with time. The settling was found to proceed roughly exponentially with time constants ranging from 10 to 60 min., depending on the particle size and concentration. The readings were taken at approximately 1 min. intervals after closing the cell and a correction to zero time was made when necessitated by rapid decay of the signals.

B. Silica Aerosol Generator

The apparatus used to generate silica aerosol is shown schematically in Figure III-2. Tetraethoxysilane (TEOS) is carried by nitrogen gas from a glass bubbler, mixed with humidifed air, and reacted in a quartz tube at 670°C. A dry ice trap removes the condensable reaction products, such as alcohols and water from the desired silica aerosol product which can be diluted with extra air and collected in a clear cylinder made of polymethylpentene. A microscope lamp (not shown) illuminates a section of the cylinder showing the presence of white smoke. A downstream pump causes the aerosol to flow from the collector to the photoacoustic cell at a constant rate and back through a water scrubber to the fume hood, which contains all the generator apparatus.

The TEOS used is 99.9999% pure from Alfa Ventron. Water bath temperature, constant for a given run, varied from 39°C to 45°C among all the runs. Nitrogen and reaction air flows were each 150 cc/min. The air stream was generally humidified, with about 1/2 the air flow passing through the water bubbler. Flows to the photoacoustic cell varied from about 1/2 to 1 1/2 ℓ/min. The dry ice trap was cleaned and dried after each run and the quartz reaction tube was so treated after every three runs. The time necessary to heat up the apparatus, establish steady state conditions and take photoacoustic data is less than two hours for each run.

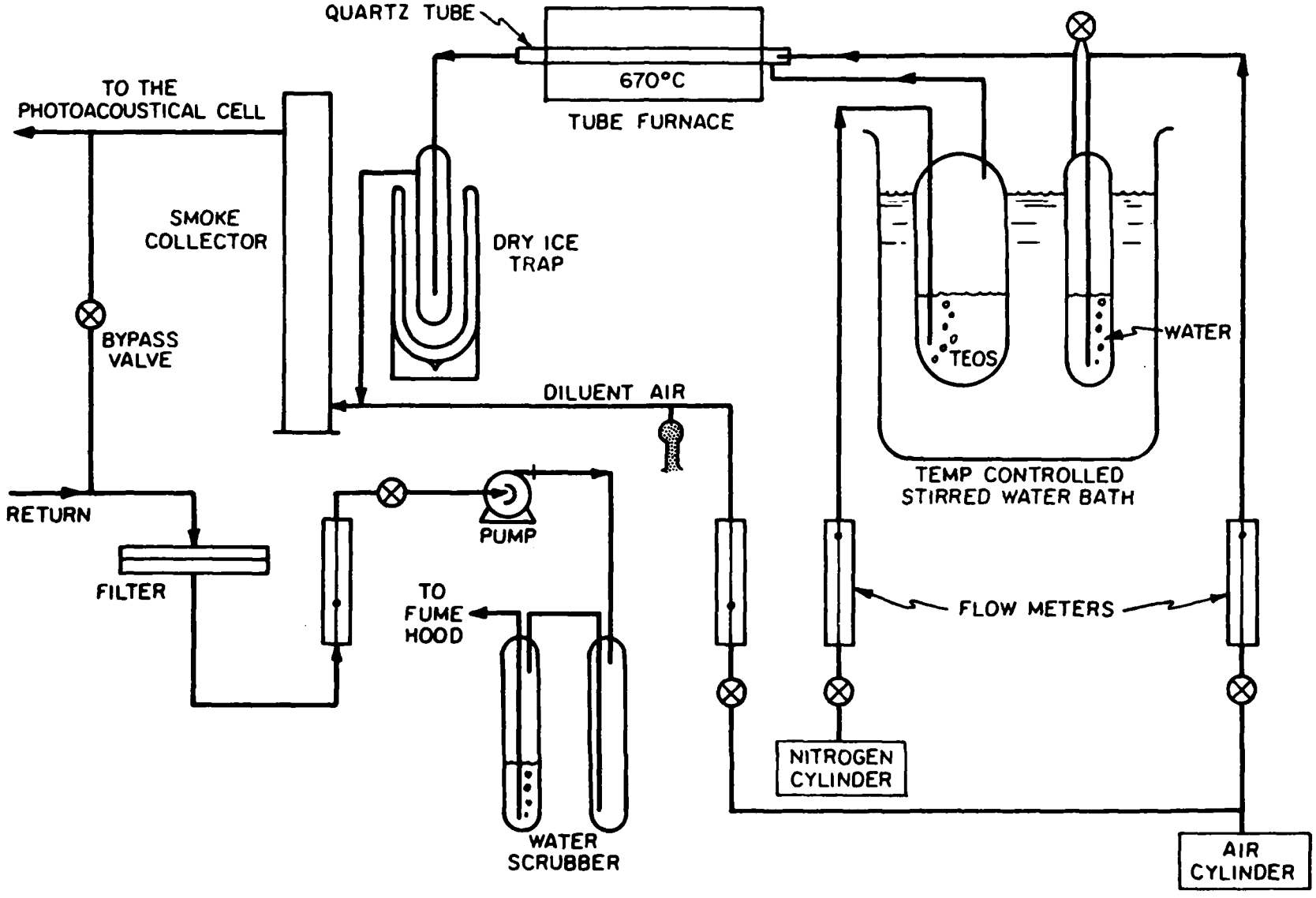

FIGURE III-2 SILICA AEROSOL GENERATOR

IV. Porosity Estimation

As mentioned in our CRDC paper the aggregate porosity is both a very important theoretical parameter and probably the most difficult parameter to characterize for an aggregate. The values of this parameter used in the CRDC paper were estimated by examination of the electron photomicrographs of relatively small aggregates or small portions of larger aggregates and extrapolation to the entire sample. Clearly, this technique is fraught with difficulties in that small aggregates tend not to include the cage-like voids seen in many larger aggregates, which however may still be small compared to the radiation wavelength. Thus the porosity would be underestimated. Beyond this is the difficulty of operator arbitrariness so that an automatic procedure, even if somewhat imperfect, would be preferable for the sake of a better comparison of results from differing samples with theory.

In a series of papers Medalia [1,2,3] made a concerted effort to obtain parameters from electron micrographs that would enable him to estimate various physical properties of the aggregates. Included in his work are the necessary factors to calculate the aggregate porosity.

Briefly, his method evolved into one which consists of assuming that the effective volume of an aggregate is the same as that of a sphere, V_{es} of the same projected area[3]. The projected area is obtained by measuring the area of the silhouette of the aggregate from an electron photomicrograph.

The volume of material within the aggregate, V_a is equal to the number of subparticles times the volume of each subparticle (assumed to be a sphere). The number of subparticles, N_p is obtained from a relationship Medalia developed in his earlier work[1,2] on randomly oriented simulated flocs. He had carried out a computer simulation by launching particles in random trajectories at an initial particle. The particles stick when they hit the growing nucleus. Comparisons of the actual number of particles in the floc and its projected area together with the projected area of the subparticles gave

$$N_P = (A/A_p)^{1.15} \qquad \text{(IV-1)}$$

where A_p is the projected area of a subparticle and A is the projected area of the aggregate (defined by the silhouette). Then the porosity

$$f_v = \frac{V_{es} - V_a}{V_{es}} \qquad \text{(IV-2)}$$

We wrote a computer program to implement both this approach and several related concepts. One of the latter we tried for fibers was to calculate the volume of an ellipsoid based on the aggregate's radius-equivalent ellipse as

$$V = \frac{4\,Ac}{3} = \frac{4\,Ab}{3} = \frac{8\,AK_b}{3} \qquad \text{(IV-3)}$$

by assuming the fiber to have a semi minor axis c equal to its semi minor b (smaller value in the micrograph) axis. Here K_b is the appropriate radius of gyration[1]. Then the porosity

$$f_v = 1 - \frac{N_p V_p}{V} = 1 - \frac{N_p \pi r_p^3}{2 A K_b} \qquad \text{(IV-4)}$$

The task of estimating the porosity of the aggregates reduces to measuring the X and Y coordinates of the boundaries of the aggregate's silhouette as well as the diameter of the subparticles. This, at least, provides a reproducible method, considerably less susceptible to photomicrograph reader errors. The computer coding is simple and the principal problems are to use a fine enough grid and to decide whether a cavity is to be considered part of the aggregate or not. The latter question clearly depends on the radiation wavelength in some fashion.

Graham[4] discussed this problem for soot particles and concluded that the Lorentz-Lorenz formula (our Effective Medium theory) is valid if:

$$\frac{2\pi a}{\lambda} \left| \tilde{m} \right| << 1 \qquad \text{(IV-5)}$$

where a is the radius of a sphere that contains many particles but is sufficiently small to satisfy the inequality, $\tilde{m}$ is the usual complex refractive index and λ the radiation wavelength. The cavities in the sample must be small compared to $\lambda/2\pi|m_a|$ where m_a is the value for the

macroscopic aggregate. For our case near 10 μm then the cavities must be much smaller than about 1 μm. This gives some guidance in drawing the particle's silhouette.

We used our new method on several runs listed in Table 1 of the CRDC paper. The results are shown in Table 3. Several points should be made. First, the revised method tends to lead to an enhanced porosity as might be expected owing to the ease with which a large (less dense) silhouette can be recorded. Also the porosities seem to tend to more similar values which may reflect on the method's improvement in removing subjectivity from the porosity estimates. Finally, however, the agreement between experimental results and theoretical simulations has been made worse. We have not been able to account for this fact. It may be that many more aggregates would have to be measured and the statistical distribution of their porosities included in the computation of scattering by the aerosol population. In our previous work we had simply assumed that the porosity of all aggregates was the same in any given experiment.

TABLE 3

CARBON AEROSOL

		AEROSOL	PARAMETERS					THEORY			EXPERIMENT		
λ	M	Shape	% Vol.	N	D	ℓ	ρ	K	S		K	S	K/S
μm	$gcm^{-3}x10^{-7}$			$cm^{-3}x10^{5}$	μm	μm	= 1-fv	cm^{-1} x 10^{-4}			cm^{-1}	x 10^{-4}	
10.5	3.3	ellip.	74		1.5		0.19	not rerun					
		sph.	17		1.1			as little					
		cyl.	9		0.36	2.4		change in fv			13.0	2.66	4.9
10.5	2.6	ellip.	50	5.0	1.3		0.11	2.35	0.0813	28.9			
		sph.	42	6.4	1.1		0.11	1.82	0.0382	47.6			
		cyl.	8	1.3	0.37	2.4	0.3	0.122	0.002	59			
								4.29	0.122	35	8.07	2.53	3.2
10.5	1.4	ellip.	66	4.0	1.45		0.11	2.35	0.102	23			
		sph.	26		1.06			not rerun					
		cyl.	8		0.38	2.4		as conclusion					
								similar			6.08	1.29	4.7

$n = 3.78$, $k = 3.15$ at $\lambda = 10.5$ μm

V. REFERENCES

1. A. I. Medalia, J. Colloid and Interface Sci. 24, 393 (1967)
2. A. I. Medalia and F. A. Heckman, Carbon 7, 567 (1969)
3. A. I. Medalia, J. Colloid and Interface Sci. 32, 115 (1970)
4. S. C. Graham, Combustion Science and Technology 9, 159 (1974)

ACKNOWLEDGEMENTS

We wish to acknowledge the scientific participation of A. G. Emslie, C. Grain, F. Johnston, Jr., F. Hatch, R. Cornish, P.C. von Thuna, and C. P. van Vloten in addition to the authors.

END

FILMED

7-85

DTIC